# Solvent-Induced Homochirality in Surface-Confined Low-Density Nanoporous Molecular Networks

Iris Destoop,[†,#] Elke Ghijsens,[†,#] Keisuke Katayama,[‡] Kazukuni Tahara,[‡] Kunal S. Mali,*,[†] Yoshito Tobe,*,[‡] and Steven De Feyter*,[†]

[†]Division of Molecular Imaging and Photonics, Department of Chemistry, KU Leuven—University of Leuven, Celestijnenlaan 200F, B 3001 Leuven, Belgium

[‡]Division of Frontier Materials Science, Graduate School of Engineering Science, Osaka University, Toyonaka, Osaka 560-8531, Japan

**S** Supporting Information

**ABSTRACT:** Induction of chirality in achiral monolayers has garnered considerable attention in the recent past not only due to its importance in chiral resolutions and enantioselective heterogeneous catalysis but also because of its relevance to the origin of homochirality in life. In this contribution, we demonstrate the emergence of macroscopic chirality in multicomponent supramolecular networks formed by achiral molecules at the interface of a chiral solvent and an achiral substrate. The solvent-mediated chiral induction provides a simple, efficient, and versatile approach for the fabrication of homochiral surfaces using achiral building blocks.

The design and fabrication of chiral surfaces has received considerable attention in the recent past due to their importance as substrates for chiral separations and enantioselective heterogeneous catalysis.[1,2] One of the simpler and rather tractable ways to construct such surfaces for chiral molecular discrimination is via supramolecular self-assembly of organic building blocks.[2−6] Due to the inherent non-centrosymmetric nature of an interface, chirality is easily achieved upon surface confinement. The exclusion of certain symmetry elements upon planar confinement ensures that even a prochiral molecule can become chiral when confined at a surface.[7] Monolayers formed by such prochiral molecules, however, remain globally achiral due to the equal amount of opposite-handed domains formed on the surface. On the other hand, for most enantiopure chiral molecules, such mirror image domains are absent, and the surface networks exhibit global organizational chirality.[2−6]

While two-dimensional (2D) self-assembly of enantiopure chiral molecules is one way to generate a homochiral surface, achiral molecules can also be forced to assemble into domains with one particular handedness, thus giving rise to a globally chiral surface. This is usually achieved by merging a small amount of chiral dopant with a supramolecular network of achiral molecules.[8−11] This ability of a few chiral molecules (*sergeants*) to control the assembly of a large number of achiral units (*soldiers*) has been termed the "sergeants-and-soldiers" principle. Similarly, a small enantiomeric excess of one enantiomer could be used to suppress the chiral expression of the other enantiomer in a so-called "majority rules" approach.[12,13] Both the "sergeants and soldiers"[14] and the "majority rules"[15] principles were pioneered by Green et al. for

solution-based systems.[13,14] Alternatively, the induction of global organizational chirality in achiral monolayers can also be realized by exposing them to magnetic fields.[16,17] Besides these chiral induction methods, the potential role of solvents in the amplification of chirality[18] and the emergence of homochirality at interfaces remains largely unexplored to date. Moreover, a majority of studies that describe chiral induction in achiral monolayers used high-density molecular networks where, within domains, molecules adsorb in a compact fashion without leaving any empty space on the surface. A nanoporous surface with chiral voids could be a potential substrate for chiral separations and catalysis.

Here we demonstrate a simple and efficient method to fabricate globally chiral nanoporous surfaces using achiral molecular building blocks by assembling them at the interface of a chiral solvent and an achiral substrate. The presence of a chiral influence in the form of an enantiopure solvent induces a clear bias toward the preferential formation of supramolecular domains with nanometer-scale voids with only one handedness. We also illustrate that, by using such enantiomorphous nanowells, it is possible to construct multicomponent homochiral networks based on host−guest interactions wherein otherwise achiral guest clusters could be confined to the surface in a chiral fashion.

We have extensively investigated the self-assembly of alkoxylated dehydrobenzo[12]annulene (DBA, Scheme 1) derivatives in the past using scanning tunneling microscopy (STM).[19] The porous networks formed by various DBAs are based on the interdigitation of alkyl chains of adjacent molecules. The relative alignment of the four interdigitated alkyl chains per DBA pair ("+" or "−" type interdigitation) governs the chirality of the resultant honeycomb network. A virtual "clockwise" (CW) or "counterclockwise" (CCW) nanowell is obtained by combining six − type or + type interdigitation patterns, respectively. The labels CW and CCW refer to the sense of rotation of the six alkyl chains making up the rim of the nanowell, and typically, the chirality of the nanowells is domain specific.[8] A relatively simple marker for the handedness of the nanowells is the relative shift of the neighboring DBA cores. The tilt of the line joining the centers of neighboring DBA cores with respect to the rim of the

**Scheme 1. Molecular Structures of Coronene (COR), Isophthalic Acid (ISA), and Dehydrobenzo[12]annulene (DBA) along with Those of the Enantiopure Solvents Used in This Study**
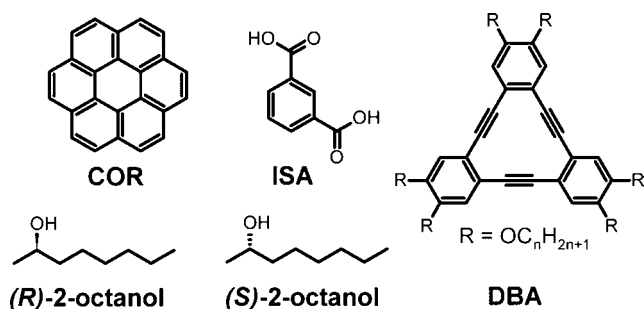


honeycomb can be used to easily identify the handedness of the network, as shown in Figure 1C,D. In the absence of any chiral influence, achiral DBA molecules (**DBA-OCn**) enantioseparate into equal amounts of mirror-image chiral domains.[9,20]
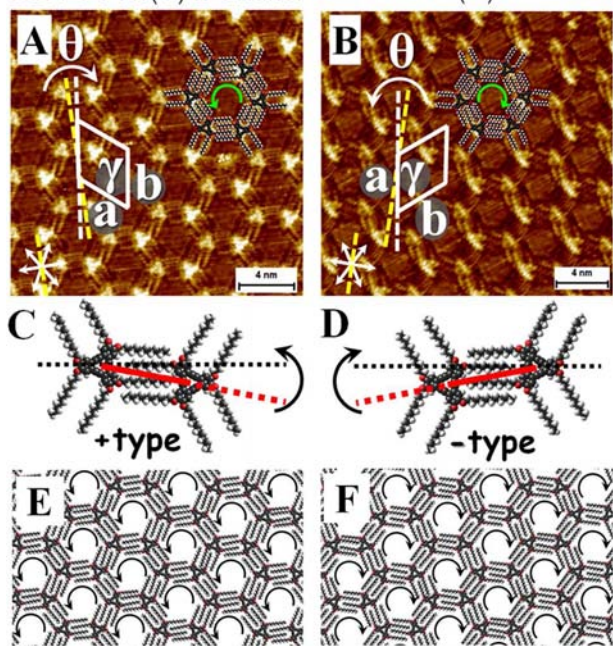


**Figure 1.** HR-STM images of the self-assembled networks of **DBA-OC10** at the (A) (S)-2-octanol/HOPG and (B) (R)-2-octanol/HOPG interface ($I_{set}$ = 280 pA, $V_{bias}$ = −230 mV). Yellow dashed lines indicate the graphite reference axis. $\theta$ is the angle between the reference axis and one of the unit cell vectors. (C,D) Markers for identifying the handedness of the molecular networks. (E,F) Molecular models for the self-assembled networks of **DBA-OC10** in (E) (S)-2-octanol and (F) (R)-2-octanol. The unit cell parameters are identical in both solvents: $a$ = 4.0 ± 0.1 nm, $b$ = 4.1 ± 0.1 nm, $\gamma$ = 61.0 ± 1.0°. For larger images, see SI.

When a solution of decyloxydehydrobenzo[12]annulene (**DBA-OC10**) in (S)-2-octanol or (R)-2-octanol is drop-casted on the basal plane of freshly cleaved highly oriented pyrolytic graphite (HOPG), a nanostructured monolayer is spontaneously formed at the liquid−solid interface. STM images (Figure 1A,B) show that **DBA-OC10** forms a honeycomb porous network at the interface of these enantiopure solvents. The plane group of this self-assembly is chiral (p6). Close

examination of STM images reveals that preferentially the + type interdigitation pattern and thus CCW honeycomb motif (94%) is obtained upon self-assembly from (S)-2-octanol. On the other hand, the self-assembly from (R)-2-octanol triggers a preferential formation of − type interdigitation pattern and hence the CW honeycomb motif (90%).

For the honeycomb networks formed from both enantiopure solvents, the induction of homochirality is also reflected in the orientation of molecular domains with respect to the graphite substrate. In the case of (S)-2-octanol, in all CCW honeycomb domains, the unit cell vectors are rotated clockwise ($\theta$ = +4.2 ± 0.5°) with respect to the reference axes $\langle 1\bar{1}00 \rangle$ of graphite. On the other hand, for all the CW honeycomb domains in (R)-2-octanol, this angle is −5.8 ± 1.3°. These preferred orientations in a given solvent clearly indicate that the enantiopure solvent governs the handedness of the molecular networks. Thus, by carrying out the self-assembly from an enantiopure chiral solvent, it is possible to induce a clear bias toward preferential formation of nanosized pores of a particular handedness. Interestingly, when adsorbed from rac-2-octanol, **DBA-OC10** forms a globally achiral surface wherein equal amounts of CW and CCW domains are formed.

An important question concerning the mechanism of chiral induction is, *At what point during the self-assembly process does the solvent transfer chiral information to the supramolecular layer?* Time-dependent STM experiments do not reveal any significant evolution of the handedness of the supramolecular network with time, indicating that the chiral induction takes place at the level of 2D nucleation via solvent−DBA and solvent−substrate interactions wherein the latter are expected to be enantiospecific. Thus, one can readily rule out the formation of racemic domains as a preceding step to the evolution of enantiopure domains. This line of thought also assumes that no chiral pre-organization takes place in solution, or that the chiral solvent molecules do not form a chiral buffer layer on graphite, on top of which the DBA molecules self-assemble. Concentration-dependent UV-absorption measurements in rac-2-octanol, ^{1}H NMR spectra in deuterated 1-octanol, and circular dichroism measurements conducted in (S)-2-octanol did not reveal any pre-organization of **DBA-OC10** in solution (see SI). Moreover, we did not find any evidence for stable self-assembly of 2-octanol molecules in the presence or absence of any of the molecules studied here. The interdigitation between the alkyl chains of DBAs leaves no space for solvent co-adsorption, and high-resolution STM data do not show any immobilized solvent molecules in the nanowells.

Another possibility is the chiral interactions between the solvent molecules in the supernatant bulk phase and the adsorbed monolayer. One possible scenario involves formation of transient complexes between the oxygen atoms of the (adsorbed) alkoxy chains of the DBA and the hydroxyl groups of the enantiopure solvents via stereospecific hydrogen-bonding interactions at the liquid−solid interface. Although this scenario cannot be ruled out entirely, a control experiment with **DBA-C10** (against that with **DBA-OC10**) indicates that such hydrogen-bonding interactions could not be solely responsible for chiral induction (Table S1).

To gain more insight into the mode of chirality transfer from chiral solvent to the DBA honeycomb network, we carried out systematic experiments probing the effect of alkoxy chain length [**DBA-OCn** ($n$ = 4, 6, 8, 10, 12, 14, 16)] and the size of the chiral solvent molecules (2-octanol versus 2-decanol).

Evaluation of the interdigitation patterns and the handedness of the nanowells reveal that all these DBA derivatives show solvent-induced homochirality. Qualitatively, the results are similar to those obtained for **DBA-OC10**. However, there are significant quantitative differences between the DBA derivatives. The shorter the alkoxy chain length, the stronger is the expression of solvent-induced chirality. A 100% chiral induction is observed for **DBA-OC6**. Moreover, 2-decanol gives rise to stronger induction effects compared to 2-octanol, especially in case of DBAs with longer alkoxy chains (Table S1).

Most likely, the chiral solvent molecules control the chiral nanowell formation by co-adsorbing along the rims of the nanowells in a dynamic fashion in the early stages of self-assembly when the nucleation begins, and it is at this stage that the chiral induction takes place. It is plausible that an adsorbed pair of DBA and 2-octanol molecules acts as a precursor for nucleation which then directs the adsorption of surrounding loosely bound DBA molecules. The fact that DBAs with shorter alkoxy chain length demonstrate greater induced chirality also highlights the important role of the structural "size matching" aspect between the enantiopure solvent and the growing DBA network. The larger the difference between the size of the solvent and the alkoxy chain of the DBA, the smaller is the induction of chirality (Figure 2 and Table S1).
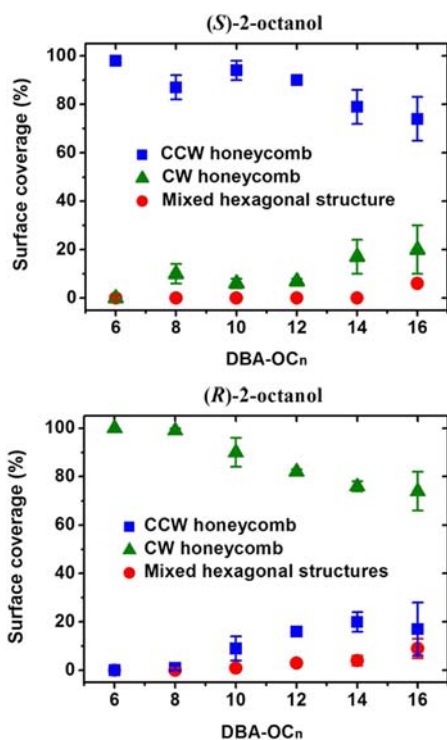
highly regular patterns; however, they offer extra challenges, as avoiding phase separation is a non-trivial issue.[20−24] STM images obtained upon drop-casting a solution containing a mixture of **DBA-OC10**, **COR**, and **ISA** in (S)-2-octanol or (R)-2-octanol on HOPG reveal that the heterocluster formed by **COR** and **ISA** in which **COR** is surrounded by six hydrogen-bonded **ISA** molecules (**COR-ISA6**) fits perfectly[20] in the nanowell formed by six molecules of **DBA-OC10** (Figure 3).



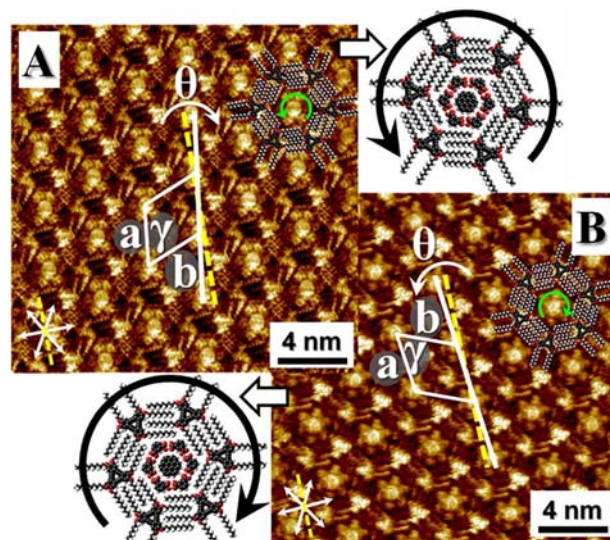**Figure 3.** HR-STM images of **DBA-OC10-COR-ISA6** (1:3:1200) on the HOPG surface from solutions of (A) (S)-2-octanol. ($I_{set}$ = 280 pA, $V_{bias}$ = −230 mV) and (B) (R)-2-octanol ($I_{set}$ = 300 pA, $V_{bias}$ = −200 mV). Molecular models showing CCW and CW honeycomb networks formed by **DBA-OC10** in which the nanowells are occupied by **COR-ISA6** are also displayed. Concentration of **DBA-OC10** = 2.1 × 10$^{-6}$ M.



**Figure 2.** Alkoxy chain length-dependent induction of 2D chirality in the honeycomb networks of DBAs, showing the population of the CW (green triangles) and the CCW (blue squares) nanowells along with that of mixed hexagonal structures (red circles).

In order to further understand the hierarchical nature of the self-assembly process and to evaluate the utility of these enantiomorphous nanowells to trap guest molecules, we examined the host−guest interactions between **DBA-OC10** network and the heteroclusters formed by coronene (**COR**) and isophthalic acid (**ISA**) (see Scheme 1) in enantiopure solvents. Such multicomponent systems are known to form

Similar to the case of a single-component **DBA-OC10** system, preferentially the + type interdigitation, and therefore also the CCW honeycomb motif (95%), is obtained upon self-assembly in (S)-2-octanol. On the other hand, the − type interdigitation pattern and hence the CW honeycomb motif (86%) is favored in (R)-2-octanol. Moreover, this global organizational chirality remains unaffected even upon evaporation of the solvent.

No chiral induction is observed when the three-component self-assembly is carried out from *rac*-2-octanol, wherein "mixed" hexagonal structures were observed apart from the usual CW and CCW honeycombs (Figure S7). The multicomponent monolayers also exhibit similar enantiospecific relation between the orientations of the molecular domains with respect to the HOPG lattice. In the case of (S)-2-octanol, in all CCW honeycomb domains, the unit cell vectors are rotated clockwise ($\theta$ = +3.7 ± 0.5°) with respect to the reference axes ⟨1$\bar{1}$00⟩ of graphite. On the other hand, for all the CW honeycomb domains in (R)-2-octanol, this angle is −4.5 ± 1.2°.

The multicomponent self-assembled networks described above clearly respond to the chirality of the solvent, and the induced handedness of the network is preserved even after the nanowells are filled with the guest heteroclusters. These results point toward a hierarchical chiral assembly mechanism. The assembly process consists of recognition between a particular handed solvent molecule (*R*- or *S*-) and the specific type of interdigitation pattern (+ or − type) followed by the occupation of the nanowells by the guest heteroclusters.

An interesting aspect of this chiral multicomponent self-assembly is that the **COR-ISA6** supramolecular network becomes enantiomorphous only upon confinement into the chiral nanowells of **DBA-OC10**. When adsorbed from enantiopure 2-octanol solvents, the two-component **COR-ISA6** system does not respond to the chirality of the solvent. The unit cell vectors of **COR-ISA6** domains formed in both enantiopure solvents are rotated both clockwise and counterclockwise ($\pm21°$ for ($S$)-2-octanol and $\pm24°$ for ($R$)-2-octanol) with respect to the reference axes $\langle1\bar{1}00\rangle$ of graphite. Mirror-image domains, which exist in equal amounts on the surface, are found in both chiral solvents, and thus the surface remains globally achiral (Figures S8−S11). This clearly indicates that the solvent-mediated chiral induction approach for the nanoporous networks could be used for trapping the guest clusters in a chiral fashion.

In conclusion, we have demonstrated, for the first time, a solvent-mediated chiral induction effect in the self-assembled monolayers of achiral building blocks giving rise to enantiomorphous nanowells. These chiral nanoporous networks could be used to host guest-clusters, creating chiral multicomponent surfaces at the liquid−solid interface. The solvent-mediated chiral induction provides a simple, efficient, and versatile approach for the fabrication of homochiral surfaces using achiral building blocks. Future work will focus on modeling of the induction effect, temperature-dependent experiments to explore kinetic versus thermodynamic effects, and experimental approaches to use these nanowells for selective trapping of a certain enantiomer from a racemic mixture.

## ■ ASSOCIATED CONTENT

### Ⓢ Supporting Information

Additional high-resolution and large-scale STM images, structural details of the monolayers, and synthesis and characterization of **DBA-OC8**. This material is available free of charge via the Internet at http://pubs.acs.org.

## ■ AUTHOR INFORMATION

### Corresponding Author

kunal.mali@chem.kuleuven.be; tobe@chem.es.osaka-u.ac.jp
Steven.DeFeyter@chem.kuleuven.be

### Author Contributions

[#]I.D. and E.G. contributed equally.

### Notes

The authors declare no competing financial interest.

## ■ ACKNOWLEDGMENTS

## ■ REFERENCES

(1) Hazen, R. M.; Sholl, D. S. *Nature* **2003**, *2*, 367−374.
(2) Pérez-Garcia, L.; Amabilino, D. B. *Chem. Soc. Rev.* **2007**, *36*, 941−967.
(3) Elemans, J. A. A. W.; De Cat, I.; Xu, H.; De Feyter, S. *Chem. Soc. Rev.* **2009**, *38*, 722−736.
(4) Raval, R. *Chem. Soc. Rev.* **2009**, *38*, 707−721.
(5) Ernst, K. H. *Top. Curr. Chem.* **2006**, *265*, 209−252.
(6) Ernst, K. H. *Curr. Opin. Colloid In. Sci.* **2008**, *13*, 54−59.
(7) Plass, K. E.; Grzesiak, A. L.; Matzger, A. J. *Acc. Chem. Res.* **2007**, *40*, 287−293.
(8) Masini, F.; Kalashnyk, N.; Knudsen, M. M.; Cramer, J. R.; Laegsgaard, E.; Besenbacher, F.; Gothelf, K. V.; Linderoth, T. R. *J. Am. Chem. Soc.* **2011**, *133*, 13910−13913.
(9) Tahara, K.; Yamaga, H.; Ghijsens, E.; Inukai, K.; Adisoejoso, J.; Blunt, M. O.; De Feyter, S.; Tobe, Y. *Nat. Chem.* **2011**, *3*, 714−719.
(10) Parschau, M.; Romer, S.; Ernst, K. H. *J. Am. Chem. Soc.* **2004**, *126*, 15398−15399.
(11) De Cat, I.; Guo, Z. X.; George, S. J.; Meijer, E. W.; Schenning, A. P. H. J.; De Feyter, S. *J. Am. Chem. Soc.* **2012**, *134*, 3171−3177.
(12) Haq, S.; Liu, N.; Humblot, V.; Jansen, A. P. J.; Raval, R. *Nat. Chem.* **2009**, *1*, 409−414.
(13) Fasel, R.; Parschau, M.; Ernst, K.-H. *Nature* **2006**, *439*, 449−452.
(14) Green, M. M.; Peterson, N. C.; Sato, T.; Teramoto, A.; Cook, R. G.; Lifson, S. *Science* **1995**, *268*, 1860−1866.
(15) Green, M. M.; Garetz, B. A.; Munoz, B.; Chang, H.; Hoke, S.; Cooks, R. G. *J. Am. Chem. Soc.* **1995**, *117*, 4181−4182.
(16) Berg, A. M.; Patrick, D. L. *Angew. Chem., Int. Ed.* **2005**, *44*, 1821−1823.
(17) Micali, N.; Engelkamp, H.; van Rhee, P. G.; Christianen, P. C. M.; Scolaro, L. M.; Maan, J. C. *Nat. Chem.* **2012**, *4*, 201−207.
(18) Katsonis, N.; Xu, H.; Haak, R. M.; Kudernac, T.; Tomovic, Z.; George, S.; Van der Auweraer, M.; Schenning, A. P. H. J.; Meijer, E. W.; Feringa, B. L.; De Feyter, S. *Angew. Chem., Int. Ed.* **2008**, *47*, 4997−5001.
(19) Tahara, K.; Lei, S.; Adisoejoso, J.; De Feyter, S.; Tobe, Y. *Chem. Commun.* **2010**, *46*, 8507−8525.
(20) Lei, S.; Surin, M.; Tahara, K.; Adisoejoso, J.; Lazzaroni, R.; Tobe, Y.; De Feyter, S. *Nano Lett.* **2008**, *8*, 2541−2546.
(21) Adisoejoso, J.; Tahara, K.; Okuhata, S.; Lei, S.; Tobe, Y.; De Feyter, S. *Angew. Chem., Int. Ed.* **2009**, *48*, 7353−7357.
(22) Madueno, R.; Raisanen, M. T.; Silien, C.; Buck, M. *Nature* **2008**, *454*, 618−621.
(23) Theobald, J. A.; Oxtoby, N. S.; Phillips, M. A.; Champness, N. R.; Beton, P. H. *Nature* **2003**, *424*, 1029−1031.
(24) Liu, J.; Chen, T.; Deng, X.; Wang, D.; Pei, J.; Wan, L. J. *J. Am. Chem. Soc.* **2011**, *133*, 21010−21015.